

# Intra-DP: A High Performance Distributed Inference System on Robotic IoT

Anonymous Author(s)

Submission Id: <PAPER ID>\*

## Abstract

The rapid advancements in machine learning (ML) techniques have led to significant achievements in various robotic tasks, where deploying these ML approaches on real-world robots requires fast and energy-efficient inference of their deep neural network (DNN) models. Distributed inference, which involves inference across multiple powerful GPU devices, has emerged as a promising optimization to improve inference performance in modern data centers. However, when deployed over Internet of Things of these real-world robots (robotic IoT), all existing parallel methods (data parallelism, tensor parallelism, pipeline parallelism) can not simultaneously meet the robots' latency and energy requirements and raise significant challenges due to the failure of data parallelism, the unacceptable communication overhead of tensor parallelism, and the significant transmission bottlenecks in pipeline parallelism. That is because existing methods are conducting layer-granulated scheduling, where the communication overhead inherent to such scheduling mechanism become significant due to the limited bandwidth of robotic IoT, and could only overlap the computation and transmission phases across multiple inferences via pipeline execution, which increases inference throughput but not the completion time of a single inference.

We present Intra-DP, the first high performance distributed inference system optimized for model inference on robotic IoT. Intra-DP confines the finer granularity of transmission and computation to each local operator of DNN layers (i.e., operators that can be computed independently without the complete input, such as the convolution kernel in the convolution layer) and schedules the transmission of each local operator adaptively to various hardware conditions and network bandwidth. In this way, different parts of the same layer can be computed and transmitted separately at the same time, which means the computation and transmission phases within the same inference task can be overlapped to achieve fast and energy-efficient distributed inference on robotic IoT. The evaluation shows that, Intra-DP reduces inference time by 10% and energy consumption by 5% compared with the state-of-the-art baselines.

## 1 Introduction

The rapid progress in machine learning (ML) techniques has led to remarkable achievements in various fundamental robotic tasks, such as object detection [18, 28, 30], robotic

control [22, 43, 53], and environmental perception [4, 23, 48]. However, deploying these ML applications on real-world robots requires fast and energy-efficient inference of their deep neural network (DNN) models, given the need for swift environmental responses and the limited battery capacity of robots. Placing the entire model on robots not only requires additional computing accelerators on robots (e.g., GPU [34], FPGA [35], SoC [15]), but also introduce additional energy consumption (e.g., 162% more for [30] in our experiments) due to the computationally intensive nature of DNN models, while placing the entire model in the cloud brings an extended response delay.

Distributed inference, which involves inference across multiple GPU devices, has emerged as a promising approach to meet the latency requirements of robotic applications and extend the battery lifetime of robots. This paradigm has been widely adopted in data centers [17, 49, 54], where numerous GPUs are utilized to speed large model inference, such as in the case of ChatGPT [47]. Adopting distributed inference across robots and other powerful GPU devices through the Internet of Things for these robots (robotic IoT) not only accelerates the inference process by leveraging the high computing capabilities of powerful GPUs but also alleviates the local computational burden, thereby reducing energy consumption, making it an ideal solution for robotic applications..

However, all existing parallel methods for distributed inference in the data center are ill-suited for robotic IoT. In data centers, there are mainly three kinds of parallel methods: Data parallelism (DP) replicates the model across devices, and lets each replica handle one mini-batch (i.e., a subset that slices out of an input data set); Tensor parallelism (TP) splits a single DNN layer over devices; Pipeline parallelism (PP) places different layers of a DNN model over devices (layer partitioning) and pipelines the inference to reduce devices' idling time (pipeline execution). In this paper, we demonstrate several issues that impede the application of existing parallel methods in robotic IoT.

For DP, the small batch sizes inherent to robotic IoT applications (typically 1) hinder the mini-batch computation, rendering DP inapplicable for robotic IoT. In the data center, DP is feasible due to the large batch sizes employed (e.g., 16 images), allowing for the division of inputs into mini-batches that still contain several complete inputs (e.g., 2 images). However, in robotic IoT, real-time performance is

111 crucial, necessitating immediate inference upon receiving inputs, which typically have smaller batch sizes (e.g., 1 image).  
 112 Further splitting these inputs would result in mini-batches  
 113 containing incomplete inputs (e.g., 1/4 of an image), which  
 114 cannot be computed parallel to speed up inference.  
 115

116 TP requires frequent synchronization among devices, leading  
 117 to unacceptable communication overhead in robotic IoT.  
 118 By partitioning parameter tensors of a layer across GPUs,  
 119 TP allows concurrent computation on different parts of this  
 120 tensor but requires an all-reduce communication [54] to  
 121 combine computation results from different devices, which  
 122 entails significant communication overhead. Consequently,  
 123 TP is used mainly for large layers that are too large to fit in  
 124 one device in data centers and require dedicated high-speed  
 125 interconnects (e.g., 400 Gbps for NVLink [21]) even within  
 126 data centers. On the contrary, robots must prioritize seam-  
 127 less mobility and primarily depend on wireless connections,  
 128 which inherently possess limited bandwidth, as described in  
 129 Sec. 2.1, making all-reduce synchronization an unacceptable  
 130 overhead (e.g., the inference time with TP was up to 143.9X  
 131 slower than local computation in our experiments).

132 Consequently, existing distributed inference approaches [5,  
 133 24] in robotic IoT primarily adopt the PP paradigm and fo-  
 134 cus on layer partitioning of PP, aiming to achieve fast and  
 135 energy-efficient inference. This is because the PP paradigm  
 136 in data centers consists of layer partitioning and pipeline  
 137 execution, where the pipeline execution of PP enhances infer-  
 138 ence throughput rather than reducing the completion time of  
 139 a single inference [6], which is the most critical requirement  
 140 in robotic IoT. Based on the fact that the amounts of output  
 141 data in some intermediate layers of a DNN model are sig-  
 142 nificantly smaller than that of its raw input data [16], DNN  
 143 layer partitioning methods constitute various trade-offs be-  
 144 tween computation and transmission, taking into account  
 145 application-specific inference speed requirements and en-  
 146 ergy consumption demands, as shown in Fig. 2.

147 Existing methods based on PP face significant challenges  
 148 due to transmission bottlenecks in robotic IoT, which are  
 149 inherent to the PP's scheduling mechanism. PP is unable to  
 150 overlap the transmission and computation phases within the  
 151 same inference to alleviate the transmission overhead, as it  
 152 can only overlap these phases across multiple inferences via  
 153 pipeline execution, which increases inference throughput  
 154 but not the completion time of a single inference [6]. Even  
 155 with optimal layer partitioning from [5, 24], such transmis-  
 156 sion overhead inherent to PP's scheduling mechanism still  
 157 becomes a substantial bottleneck due to the limited band-  
 158 width of robotic IoT (e.g., up to 69% of inference time in our  
 159 experiments).

160 The key reason is that existing methods can not overlaps  
 161 the computation and transmission phases within the existing  
 162 PP's layer partitioning framework which has the potential  
 163 to address the shortcomings of current distributed inference  
 164

166 approaches. Regarding the overlapping of communication  
 167 costs within a single inference task, since transmission time  
 168 constitutes a significant portion of the total inference time  
 169 (approximately half) in existing PP's layer partitioning, a  
 170 novel parallel method that overlaps the computation and  
 171 transmission phases has significant potential for optimiz-  
 172 ing and speeding up inference time. Furthermore, it is es-  
 173 sential to recognize that transmission energy consumption  
 174 encompasses the energy used by the device during the data  
 175 transmission phase, not merely the energy expended for the  
 176 transmission itself (such as that by the wireless network  
 177 card). The comparison of transmission and standby energy  
 178 consumption in Tab. 3 also indicates that wireless network  
 179 cards consume only 0.21W during our experiments. This  
 180 suggests that overlapping the two phases will not signifi-  
 181 cantly increase the energy consumption during the robot  
 182 computation phase but will reduce the robot's waiting time  
 183 for the final inference result during the data transmission  
 184 phase, thereby decreasing overall energy consumption. By  
 185 implementing this method, we can achieve faster and more  
 186 energy-efficient inference, facilitating more effective deploy-  
 187 ment of DNN models on robotic IoT.

188 observation: local operator

189 challenge:

190 intra-data DP

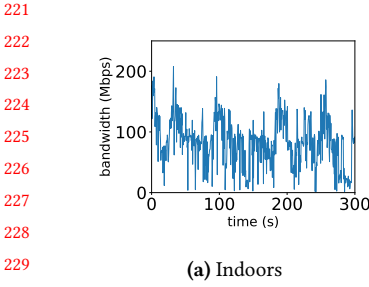
191 how to optimal? Nonlinear optimization problem

## 2 Background

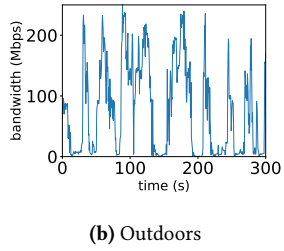
### 2.1 Characteristics of Robotic IoT

195 In real-world robotic IoT scenarios, devices often navigate  
 196 and move around for tasks like search and exploration. While  
 197 wireless networks provide high mobility, they also have lim-  
 198 ited bandwidth. For instance, Wi-Fi 6, the most advanced  
 199 Wi-Fi technology, offers a maximum theoretical bandwidth  
 200 of 1.2 Gbps for a single stream [27]. However, not only the  
 201 limited hardware resources on the robot can not fully play  
 202 the potential of Wi-Fi 6 [52], but also the actual available  
 203 bandwidth of wireless networks is often reduced in practice  
 204 due to factors such as movement of the devices [29, 36], oc-  
 205 clusion from by physical barriers [8, 38], and preemption of  
 206 the wireless channel by other devices [2, 37].

207 To demonstrate the instability of wireless transmission  
 208 in real-world situations, we conducted a robot surveillance  
 209 experiment using four-wheel robots navigating around sev-  
 210 eral given points at 5-40cm/s speed in our lab (indoors) and  
 211 campus garden (outdoors), with hardware and wireless net-  
 212 work settings as described in Sec. 4. We believe our setup  
 213 represents robotic IoT devices' state-of-the-art computation  
 214 and communication capabilities. We saturated the wireless  
 215 network connection with iperf [1] and recorded the average  
 216 bandwidth capacity between these robots every 0.1s for 5  
 217 minutes.



(a) Indoors



(b) Outdoors

**Figure 1.** The instability of wireless transmission in robotic IoT networks.

The results in Fig. 1 show average bandwidth capacities of 93 Mbps and 73 Mbps for indoor and outdoor scenarios, respectively. The outdoor environment exhibited higher instability, with bandwidth frequently dropping to extremely low values around 0 Mbps, due to the lack of walls to reflect wireless signals and the presence of obstacles like trees between communicating robots, resulting in fewer received signals compared to indoor environments.

In summary, robotic IoT systems' wireless transmission is constrained by limited bandwidth, both due to the theoretical upper limit of wireless transmission technologies and the practical instability of wireless networks.

## 2.2 Characteristics of Data Center Networks

Data center networks, which are used for large model inference (e.g., ChatGPT [47]), are wired and typically exhibit higher bandwidth capacity and lower fluctuation compared to robotic IoT networks. GPU devices in data centers are interconnected using high-speed networking technologies such as InfiniBand [42] or PCIe [21], offering bandwidths ranging from 40 Gbps to 500 Gbps. The primary cause of bandwidth fluctuation in these networks is congestion on intermediate switches, which can be mitigated through traffic scheduling techniques implemented on the switches [33]. The stable and high-bandwidth nature of data center networks makes them well-suited for demanding tasks like large model inference, in contrast to the more variable and resource-constrained environments found in robotic IoT networks.

## 2.3 Existing distributed inference strategies in the data center

**Data parallelism.** Data parallelism [49] is a widely used technique in distributed inference that partitions input data across multiple devices, such as GPUs, to perform parallel inference. Each device maintains a complete model replica and independently processes a subset of the input data (mini-batch), aggregating results to generate the final output. Data parallelism enhances throughput by distributing workload

across devices, leveraging their combined computational power.

However, data parallelism's scalability is constrained by the total batch size [32], which is particularly problematic in robotic IoT applications where smaller batch sizes are inherent due to the need for swift environmental responses. In robotic applications, immediate inference upon receiving inputs is crucial for obtaining real-time target points quickly. For example, in our experiments, the robot constantly obtains the latest images from the camera for inference, with a batch size of only 1. These small batches cannot be further split into mini-batches, a fundamental requirement for effective data parallelism.

**Tensor parallelism.** Tensor parallelism [54] is a distributed inference technique that divides a model's layer parameters across multiple devices, each storing and computing a portion of the weights. This approach requires an all-reduce communication step after each layer to combine results from different devices, introducing significant overhead, especially for large DNN layers. To mitigate this, TP is typically deployed across GPUs within the same server in data centers, using fast intra-server GPU-to-GPU links like NVLink [21], which is beneficial when the model is too large for a single device.

In contrast to data center networks, the limited bandwidth in robotic IoT (see Sec. 2.1) renders the communication cost of TP prohibitively high. Our experiments demonstrate that the all-reduce communication cost of TP can consume up to 94% of the total inference time, leading to a upper to 143.9x increase in inference time and 62.7x higher energy consumption per inference compared to computing the entire model locally on the robot (see Sec.??). Such significant overhead introduced by TP's communication requirements makes it impractical for deployment in bandwidth-constrained robotic IoT environments.

We chose a state-of-the-art tensor parallelism method, DINA [31], as our baseline; Table 1 reveals that transmission time constitutes 49% to 94% of total inference time due to all-reduce communication for each layer, resulting in TP's inference time being 45.2X to 143.9X longer than local computation. Although Table 2 indicates lower power consumption with TP (13.4% to 67.3% less than local computation, because TP spent much more time on transmission when have lower power consumption in Tab.3), the extended transmission times significantly increase energy consumption per inference, ranging from 28.5X to 62.7X. Since TP significantly extends inference time, making it impractical for real-world robotic applications that require real-time control, we did not further evaluate TP in these contexts.

**Pipeline parallelism.** Pipeline parallelism [17] is a distributed inference technique that partitions DNN model layers across multiple devices(layer partitioning), forming an inference pipeline for concurrent processing of multiple tasks.

Model(number of parameters)	Local computation time(s)	Environment	Transmission time (s) with TP	Inference time (s) with TP	Percentage(%) with TP
MobileNet_V3_Small(2M)	0.031( $\pm 0.004$ )	indoors	0.698( $\pm 0.135$ )	1.400( $\pm 0.232$ )	49.85
		outdoors	0.901( $\pm 0.778$ )	1.775( $\pm 1.370$ )	51.23
ResNet101(44M)	0.065( $\pm 0.005$ )	indoors	7.156( $\pm 3.348$ )	8.106( $\pm 3.403$ )	87.95
		outdoors	8.470( $\pm 6.337$ )	9.356( $\pm 6.328$ )	90.46
VGG19_BN(143M)	0.063( $\pm 0.002$ )	indoors	5.152( $\pm 4.873$ )	5.444( $\pm 4.831$ )	70.18
		outdoors	5.407( $\pm 6.673$ )	5.759( $\pm 6.635$ )	93.70

**Table 1.** Average transmission time (Second), inference time (Second), percentage that transmission time accounts for of inference time and their standard deviation ( $\pm n$ ) with TP on different models in different environments. “Local computation” refers to placing the whole layers on the robot.

Model(number of parameters)	Environment	Power consumption(W)		Energy consumption(J) per inference	
		Local	TP	Local	TP
MobileNet_V3_Small(2M)	indoors	6.05( $\pm 0.21$ )	5.24( $\pm 0.19$ )	0.3( $\pm 0.09$ )	7.33( $\pm 1.21$ )
	outdoors	6.05( $\pm 0.21$ )	5.11( $\pm 0.28$ )	0.3( $\pm 0.09$ )	9.08( $\pm 7.0$ )
ResNet101(44M)	indoors	11.27( $\pm 0.51$ )	4.97( $\pm 0.16$ )	0.93( $\pm 0.19$ )	40.28( $\pm 16.91$ )
	outdoors	11.27( $\pm 0.51$ )	4.9( $\pm 0.23$ )	0.93( $\pm 0.19$ )	45.8( $\pm 30.98$ )
VGG19_BN(143M)	indoors	14.86( $\pm 0.43$ )	4.88( $\pm 0.29$ )	1.19( $\pm 0.18$ )	26.55( $\pm 23.56$ )
	outdoors	14.86( $\pm 0.43$ )	4.87( $\pm 0.27$ )	1.19( $\pm 0.18$ )	28.06( $\pm 32.33$ )

**Table 2.** Power consumption against time (Watt) and energy consumption per inference (Joule) with standard deviation ( $\pm n$ ) with TP on different models in different environments. “Local” represents “Local computation”

While PP can increase throughput and resource utilization via pipeline execution, it primarily focuses on enhancing overall throughput rather than reducing single-inference latency [6], which is crucial in robotic IoT. As a result, existing distributed inference approaches [5, 24] in robotic IoT mainly concentrate on the layer partitioning aspect of PP, aiming to achieve fast and energy-efficient inference by optimizing the allocation of DNN layers across devices while considering factors such as device capabilities, network bandwidth, and energy consumption, as discussed further in Sec. 3.1.

## 2.4 Other methods to speed up DNN Models Inference on Robotic IoT

**Compressed communication.** Compressed communication is crucial for efficient distributed inference in wireless networks, as it significantly reduces communication overhead through techniques such as quantization and model distillation. Quantization [7, 11, 12] is a technique that reduces the numerical precision of model weights and activations, thereby minimizing the memory footprint and computational requirements of deep learning models. This process typically involves converting high-precision (e.g., 32-bit) floating-point values to lower-precision (e.g., 8-bit) floating-point representations, with minimal loss of model accuracy. Model distillation [13, 26, 44], on the other hand, is an approach that involves training a smaller, more efficient “student” model to mimic the behavior of a larger, more accurate “teacher” model by minimizing the difference between the student model’s output and the teacher model’s output. The distilled student model retains much of

the teacher model’s accuracy while requiring significantly fewer resources. These model compression methods complement distributed inference by achieving faster inference speed through model modifications, potentially sacrificing some accuracy with smaller models, while distributed inference realizes fast inference without loss of accuracy by intelligently scheduling computation tasks across multiple devices. Moreover, given the requirement to maintain the integrity of the final inference results, intermediate results cannot be altered during transmission. Consequently, only lossless compression methods [14] can be utilized to reduce the transmission volume.

**Inference Job scheduling.** Significant research efforts have been devoted to exploring inference parallelism and unleashing the potential of layer partition to accelerate DNN inference, such as inference job scheduling, aiming to accelerate multiple DNN inference tasks by optimizing their execution on various devices under different network bandwidths while considering application-specific inference speed requirements and energy consumption demands. For instance, [3, 9] support online scheduling of offloading inference tasks based on the current network and resource status of mobile systems while meeting user-defined energy constraints. [10] focused on optimizing DNN inference workloads in cloud computing using a deep reinforcement learning based scheduler for QoS-aware scheduling of heterogeneous servers, aiming to maximize inference accuracy and minimize response delay. While these methods focus on overall optimization in multi-task scenarios involving multi-robots, they do not address the optimization of single inference tasks and are thus

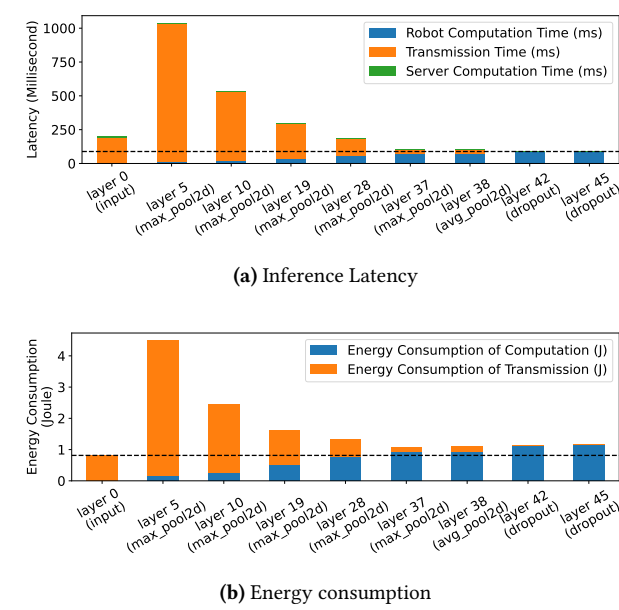


**Figure 2.** Our experiments on VGG19 [39] reveal the comprehensive performance of various layer partitioning methods. The X-axis of the graph represents different layer partitioning scheduling schemes, where 'layer i' signifies that all layers up to and including the i-th layer are computed on the robot, while the subsequent layers are processed on the GPU devices. Note that different hardware conditions, network conditions and DNN model structure will lead to different performance, making this field an attractive area for a wide range of research.

orthogonal to distributed inference for a single inference, where improved distributed inference can provide faster and more energy-efficient inference for these scenarios.

### 3 Problems in Existing Distributed Inference for DNN Models on Robotic IoT

#### 3.1 Existing distributed inference on robotic IoT

Existing distributed inference approaches [5, 24] in robotic IoT primarily adopt the PP paradigm and focus on layer partitioning to achieve fast and energy-efficient inference. These approaches can be divided into two main categories based on their optimization goals: accelerating inference for diverse DNN structures and optimizing robot energy consumption during inference.

To accelerate inference, earlier methods [16, 19, 31] focused on simple chain-like DNN models by exploiting the smaller output data sizes of intermediate layers compared to raw input data [16], creating trade-offs between computation and transmission to minimize overall inference time (see Fig. 2). However, the increasing complexity of DNN structures, now evolved into directed acyclic graphs (DAGs),

poses new challenges, potentially leading to NP-hardness in performance optimization [24]. This issue is addressed by graph theory techniques [24, 51] and varying hardware and network conditions further complicate the problem.

To optimize energy consumption, existing methods [5, 25, 46] build upon the aforementioned techniques and consider reducing the system energy consumption of the entire layer partitioning execution process under deadline constraints. While [46] only considers transmission energy consumption, [5, 25] aim to reduce the whole system's energy consumption during DNN layer execution and data transfer.

In summary, these two categories primarily adopt the PP paradigm but suffer from the transmission bottleneck inherent to PP's scheduling mechanism (see Sec. 3.2). Consequently, achieving fast and energy-efficient inference on robotic IoT remains an open issue.

#### 3.2 Dilemma on Inference Time and Energy Consumption

Regardless of the complexity of DNN models, layer partitioning methods consist of three phases: computing earlier DNN layers on robots, transmitting intermediate results, and completing inference on the GPU device. Since the GPU device's computation time is negligible compared to the other two phases (see Fig. 2) due to the high computing capabilities of GPU devices, this paper focuses on the computation phase of robots and the data transmission phase via robotic IoT.

The data transmission phase can only begin after obtaining the calculation result of the intermediate layer when the computation phase on robots is completed, preventing overlap for a single inference task. PP can only overlap computation and data transmission phases from different inference tasks, not from the same task [6]. However, the transmission cost inherent to the PP's scheduling mechanism becomes a bottleneck in robotic IoT due to limited bandwidth. In our experiments, even with optimal layer partitioning [5, 24], such communication cost takes up to 63% of inference time.

To make matters worse, such transmission overhead not only leads to prolonged inference time but also to high energy consumption during the data transmission phase, referred to as transmission energy consumption. Our findings reveal that such transmission energy consumption accounts for nearly one-third of the total energy consumed during inference (see Sec.??). This is because the device cannot be put into low-power sleep mode while waiting for the final inference result from the GPU device, as it has to promptly continue working when it receives the inference results. Moreover, chips like CPU, GPU, and memory consume non-negligible power even when not computing, due to the static power consumption rooted in transistors' leakage current [20]. Consequently, both the energy consumed during the execution of DNN layers on robots, referred to as robot

computation energy consumption, and the transmission energy consumption resulting from prolonged transmission times substantially impact the overall power consumption of the inference process in robotic IoT.

Only models with limited transmission overhead can mitigate the impact of these shortcomings on inference performance. However, the unstable bandwidth in robotic IoT wireless networks can cause the transmission time for layer partitioning to vary dramatically, sometimes changing by hundreds of times (see Fig. 1). In our experiments, even a relatively small model with only 0.84M parameters still suffers from its significant transmission overhead. The significant impact of transmission overhead on both inference time and energy consumption highlights the need for innovative approaches that can effectively mitigate the transmission bottleneck in robotic IoT.

### 3.3 Special Cases

Since layer partitioning methods schedule at the granularity of model layers, “local computation” and “edge computation” are special cases of layer partitioning. “Local computation” refers to placing the whole layers on the robot when the bandwidth is too low, while “edge computation” means placing the whole layers on GPU devices when the bandwidth is sufficient. Local computation avoids the impact of network transmission on inference time but consumes the maximum computation energy consumption. On the other hand, edge computation minimizes computation energy consumption but requires a high enough bandwidth to ensure the lowest possible transmission energy consumption and overall inference time. These two special cases are indispensable for existing methods to cope with different network conditions, when they are too low or sufficient, and to address the need for various trade-offs between inference delay and energy consumption.

In our experiments, we found that the bandwidth conditions under which the layer partitioning scheme of different models becomes these special cases vary, and the higher the bandwidth, the more layers are scheduled to be placed on GPU devices. We explain the reasons causing different bandwidth conditions for different models in Sec. ?? with some detailed real-world cases. The existence of these special cases highlights the importance of considering the relationship between bandwidth, model structure, and the resulting trade-offs between inference delay and energy consumption.

## 4 Evaluation

**Testbed.** The evaluation was conducted on a custom four-wheeled robot (Fig 3a), and a custom air-ground robot (Fig 3b). They are equipped with a Jetson Xavier NX [34] 8G onboard computer that is capable of AI model inference with local computation resources. The system runs Ubuntu 20.04 with ROS Noetic and a dual-band USB network card (MediaTek

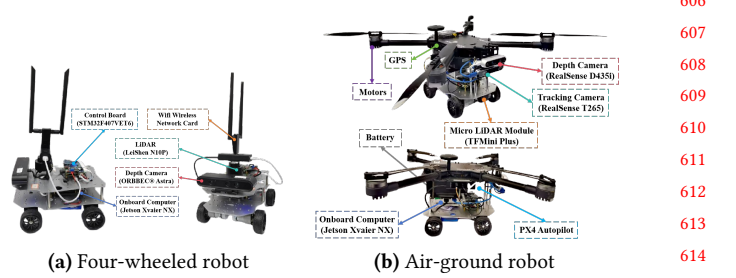


**Figure 3.** The detailed composition of the robot platforms

	inference	transmission	standby
Power (W)	13.35	4.25	4.04

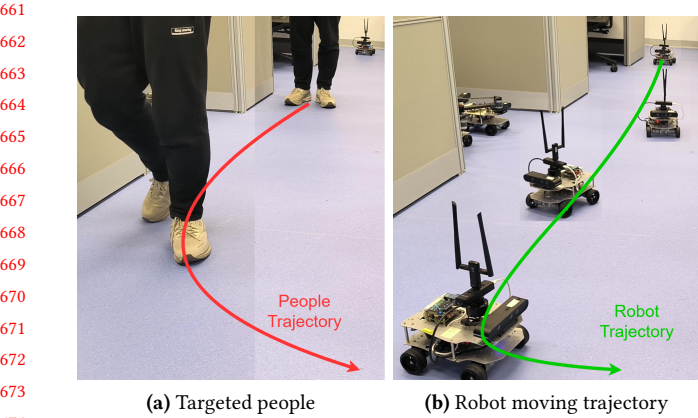
**Table 3.** Power consumption (Watt) of our robot in different states.

MT76x2U) for wireless connectivity. The Jetson Xavier NX interfaces with a Leishen N10P LiDAR, ORBBEC Astra depth camera, and an STM32F407VET6 controller via USB serial ports. Both LiDAR and depth cameras facilitate environmental perception, enabling autonomous navigation, obstacle avoidance, and SLAM mapping. The GPU server accepting offloaded computation tasks from the robot is a PC equipped with an Intel(R) i5 12400f CPU @ 4.40GHz and an NVIDIA GeForce GTX 2080 Ti 11GB GPU, connected to our robot via WiFi 6 over 80MHz channel at 5GHz frequency in our experiments.

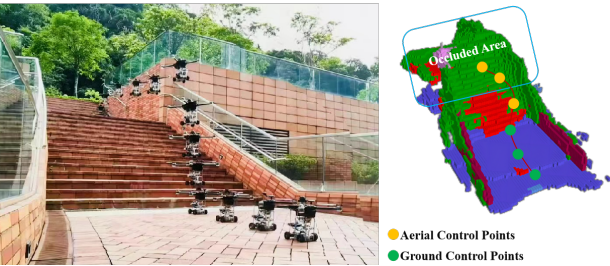
Tab. 3 presents the overall on-board energy consumption (excluding motor energy consumption for robot movement) of the robot in various states: inference (model inference with full GPU utilization, including CPU and GPU energy consumption), transmission (communication with the GPU server, including wireless network card energy consumption), and standby (robot has no tasks to execute). Notice that different models, due to varying numbers of parameters, exhibit distinct GPU utilization rates and power consumption during inference.

We evaluated two real-world environments: indoors (robots move in our laboratory with desks and separators interfering with wireless signals) and outdoors (robots move in our campus garden with trees and bushes interfering with wireless signals, resulting in lower bandwidth). The corresponding bandwidths between the robot and the GPU server in indoors and outdoors scenarios are shown in Fig. 1.

**Workload.** We evaluated two typical real-world robotic applications on our testbed: Kapao, a real-time people-tracking application on our four-wheeled robot (Fig 4), and AGRNav, an autonomous navigation application on our air-ground robot (Fig 5). These applications feature different model input and output size patterns: Kapao takes RGB images as input and outputs key points of small data volume. In contrast, AGRNav takes point clouds as input and outputs predicted



675 **Figure 4.** A real-time people-tracking robotic application  
676 on our robot based on a well-known human pose estimation  
677 ML model, Kapao [30].



688 **Figure 5.** By predicting occlusions in advance, AGRNav [43]  
689 gains an accurate perception of the environment and avoids  
690 collisions, resulting in efficient and energy-saving paths.

691 point clouds and semantics of similar data volume as input,  
692 implying that AGRNav needs to transmit more data during  
693 offloading. And we have verified several models common  
694 to mobile devices on a larger scale to further corroborate  
695 our observations and findings: MobileNet [40], ResNet [41],  
696 VGGNet [39], ConvNeXt [45], RegNet [50].

697 **Baselines.** We selected two SOTA pipeline parallelism  
698 methods as baselines: DSCCS [24], aimed at accelerating  
699 inference, and SPSO-GA [5], focused on optimizing energy  
700 consumption. We set SPSO-GA's deadline constraints to 1 Hz,  
701 the minimum frequency required for robot movement control.  
702 Given our primary focus on inference time and energy  
703 consumption per inference, we disabled pipeline execution to  
704 concentrate solely on assessing the performance of various  
705 layer partitioning methods.

#### 707 4.1 Inference Time

709 **Kapao.** From the results in the upper part of Tab. 4, both  
710 SPSO-GA and DSCCS reduced Kapao's inference time by  
711 39.69% and 56.92% indoors and 28.67% and 47.46% outdoors,  
712 with DSCCS achieving 28.57% (indoors) and 26.34% (out-  
713 doors) lower inference time than SPSO-GA. While both  
714 systems significantly reduced inference time via offloading,

715 transmission time accounts for 49.69% to 69.46% of the whole  
716 inference time, indicating that even with SOTA layer parti-  
717 tioning, the transmission bottleneck inherent to PP's schedul-  
718 ing mechanism cannot be mitigated. The difference between  
719 DSCCS and SPSO-GA can be attributed to their optimiza-  
720 tion goals: DSCCS minimizes inference latency, while SPSO-GA  
721 minimizes power consumption under deadline constraints.

722 **AGRNav.** The performance gain of the two offloading  
723 systems varied for AGRNav, as shown in the lower part of  
724 Tab. 4. DSCCS still reduced inference time by 18.34% and  
725 12.43% in indoors and outdoors. However, SPSO-GA achieved  
726 similar inference time (3.65% and 3.06% reduction) as local  
727 computation both indoors and outdoors. We will explain and  
728 analyze this phenomenon in Sec.4.2.

729 Notice that the large standard deviation in transmission  
730 time in outdoors in both offloading systems indicates that  
731 bandwidth fluctuated more frequently and more fiercely out-  
732 doors compared with indoors, which complies with Fig. 1.  
733 Additionally, the lower average bandwidth for outdoors sce-  
734 narios (see Sec.2.1) results in increased transmission and  
735 inference times relative to indoor scenarios.

#### 736 4.2 Breakdown

737 Both SPSO-GA and DSCCS automatically adapt to available  
738 bandwidth, transitioning to edge computation (placing all  
739 DNN layers on the GPU server) when bandwidth is suffi-  
740 cient, and to local computation (placing all DNN layers on  
741 robots) when bandwidth is low. To better understand how  
742 their layer partitioning scheduling varies with different net-  
743 work conditions and models, we recorded and analyzed the  
744 Categories and percentages of various layer partitioning  
745 schedules under different baselines and environments, as  
746 detailed in Fig. 6.

747 Local computation and edge computation are special cases  
748 of layer partitioning, with the bandwidth conditions required  
749 for each model to reach these cases varying based on the  
750 model structure and partitioning method used. Analyzing  
751 Fig. 6a and Fig. 6b, both SPSO-GA and DSCCS tend to allocate  
752 more layers on the robot for AGRNav. When comparing  
753 indoor and outdoor scenarios in Fig. 6, it is evident that  
754 higher bandwidth leads to more layers being scheduled on  
755 GPU server. Additionally, when comparing SPSO-GA and  
756 DSCCS in Fig. 6, DSCCS, which focuses on optimizing energy  
757 consumption, tends to place fewer layers on the robot to  
758 reduce computation energy consumption.

759 In summary, the conditions under which layer partitioning  
760 schemes make these special cases are influenced by multiple  
761 factors: model structure, and the trade-offs between infer-  
762 ence delay and energy consumption. And the higher the  
763 bandwidth, the more layers are scheduled to be placed on  
764 GPU server.

Model(number of parameters)	Local computation time (s)	Environment	Transmission time (s)		Inference time (s)		Percentage(%)	
			SPSO-GA	DSCCS	SPSO-GA	DSCCS	SPSO-GA	DSCCS
Kapao(77M)	0.708( $\pm 0.023$ )	indoors	0.212( $\pm 0.085$ )	0.204( $\pm 0.088$ )	0.427( $\pm 0.122$ )	0.305( $\pm 0.113$ )	49.69	66.68
		outdoors	0.271( $\pm 0.563$ )	0.259( $\pm 0.531$ )	0.505( $\pm 0.573$ )	0.372( $\pm 0.535$ )	53.49	69.46
AGRNav(0.84M)	1.014( $\pm 0.034$ )	indoors	0.273( $\pm 0.166$ )	0.133( $\pm 0.793$ )	0.977( $\pm 0.32$ )	0.828( $\pm 0.646$ )	28.04	15.99
		outdoors	0.177( $\pm 0.762$ )	0.089( $\pm 0.085$ )	0.983( $\pm 0.759$ )	0.888( $\pm 0.067$ )	17.93	10.02

**Table 4.** Average transmission time (Second), inference time (Second), percentage that transmission time accounts for of inference time and their standard deviation ( $\pm n$ ) of Kapao and AGRNav with different pipeline parallelism offloading systems and different environments. “Local computation” refers to placing the whole layers on the robot.

Model(number of parameters)	Environment	Power consumption(W)			Energy consumption(J) per inference			SPSO-GA	DSCCS
		Local	SPSO-GA	DSCCS	Local	SPSO-GA	DSCCS		
Kapao(77M)	indoors	15.03( $\pm 0.63$ )	6.21( $\pm 2.76$ )	6.42( $\pm 3.09$ )	9.26( $\pm 0.2$ )	1.95( $\pm 0.76$ )	1.23( $\pm 0.71$ )	838	839
	outdoors	15.03( $\pm 0.63$ )	7.91( $\pm 4.2$ )	8.07( $\pm 4.35$ )	9.26( $\pm 0.2$ )	2.92( $\pm 4.53$ )	1.95( $\pm 4.32$ )		
AGRNav(0.84M)	indoors	10.82( $\pm 1.44$ )	6.47( $\pm 2.06$ )	10.43( $\pm 2.4$ )	10.97( $\pm 0.37$ )	2.95( $\pm 1.93$ )	4.48( $\pm 6.71$ )	840	841
	outdoors	10.82( $\pm 1.44$ )	8.77( $\pm 3.07$ )	10.78( $\pm 1.47$ )	10.97( $\pm 0.37$ )	4.7( $\pm 6.62$ )	4.97( $\pm 0.47$ )		

**Table 5.** The power consumption against time (Watt) and energy consumption per inference (Joule) with standard deviation ( $\pm n$ ) of Kapao and AGRNav at different baselines and environments. “Local” represents “Local computation”

Model(number of parameters)	Local computation time (s)	Environment	Transmission time (s)		Inference time (s)		Percentage(%)	
			SPSO-GA	DSCCS	SPSO-GA	DSCCS	SPSO-GA	DSCCS
MobileNet_V3_Small (2M)	0.033( $\pm 0.019$ )	indoors	0.035( $\pm 0.019$ )	0.016( $\pm 0.005$ )	0.044( $\pm 0.020$ )	0.031( $\pm 0.008$ )	79.79	53.24
		outdoors	0.035( $\pm 0.044$ )	0.017( $\pm 0.005$ )	0.047( $\pm 0.037$ )	0.033( $\pm 0.018$ )	50.04	51.49
RegNet_X_3_2GF (15M)	0.060( $\pm 0.022$ )	indoors	0.049( $\pm 0.026$ )	0.033( $\pm 0.011$ )	0.065( $\pm 0.028$ )	0.049( $\pm 0.016$ )	76.25	64.17
		outdoors	0.049( $\pm 0.055$ )	0.032( $\pm 0.032$ )	0.069( $\pm 0.050$ )	0.051( $\pm 0.030$ )	53.23	44.50
ResNet101 (44M)	0.060( $\pm 0.023$ )	indoors	0.054( $\pm 0.451$ )	0.033( $\pm 0.010$ )	0.072( $\pm 0.453$ )	0.050( $\pm 0.016$ )	75.64	57.37
		outdoors	0.052( $\pm 0.064$ )	0.033( $\pm 0.036$ )	0.077( $\pm 0.059$ )	0.054( $\pm 0.034$ )	51.54	42.48
ConvNeXt_Base (88M)	0.047( $\pm 0.004$ )	indoors	0.033( $\pm 0.018$ )	0.020( $\pm 0.006$ )	0.044( $\pm 0.019$ )	0.032( $\pm 0.009$ )	75.39	49.37
		outdoors	0.032( $\pm 0.038$ )	0.020( $\pm 0.022$ )	0.045( $\pm 0.033$ )	0.034( $\pm 0.019$ )	52.82	35.63
ConvNeXt_Large (197M)	0.051( $\pm 0.005$ )	indoors	0.033( $\pm 0.017$ )	0.023( $\pm 0.008$ )	0.046( $\pm 0.019$ )	0.035( $\pm 0.013$ )	72.96	62.68
		outdoors	0.032( $\pm 0.038$ )	0.023( $\pm 0.024$ )	0.054( $\pm 0.040$ )	0.041( $\pm 0.028$ )	48.94	43.96
RegNet_Y_128GF (644M)	0.139( $\pm 0.016$ )	indoors	0.076( $\pm 0.289$ )	0.041( $\pm 0.024$ )	0.305( $\pm 0.382$ )	0.100( $\pm 0.035$ )	23.58	40.76
		outdoors	0.171( $\pm 0.602$ )	0.016( $\pm 0.055$ )	0.432( $\pm 0.615$ )	0.117( $\pm 0.242$ )	32.39	9.41

**Table 6.** Average transmission time (Second), inference time (Second), percentage that transmission time accounts for of inference time and their standard deviation ( $\pm n$ ) of common AI models in different environments with different offloading systems. “Local computation” refers to placing the whole layers on the robot.

### 4.3 Energy Consumption

**Kapao.** From the results in the upper part of Tab. 5, DSCCS consumed 3.38% and 2.02% more power per second than SPSO-GA indoors and outdoors due to more layers placed on robots shown in Fig. 6a. However, SPSO-GA consumed 58.54% and 49.74% more energy overall to process a frame than DSCCS because it only aims at minimizing the power consumption against time at the cost of possibly prolonged inference time.

**AGRNav.** From the results in the lower part of Tab. 5, DSCCS consumed 61.21% and 22.92% more energy per second than SPSO-GA indoors and outdoors ( Tab. 5), while DSCCS consumed 34.15% and 5.43% more energy to process a frame than SPSO-GA. SPSO-GA’s advantages in power consumption aganist time shrinks in energy consumption per inference due to prolonged inference time.

### 4.4 Validation on a larger range of models

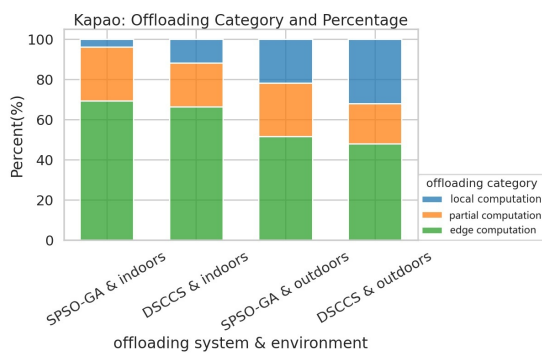
We evaluated PP across a broad range of models with varying parameter counts (from 0.84M to 644M, as detailed in Tab. 6 and Tab. 7), which are commonly used in mobile devices. Our findings confirm that transmission time constitutes a significant portion of the total inference time in robotic IoT when using PP. The inherent transmission overhead of PP’s scheduling mechanism significantly wastes both inference time and energy.

## 5 Conclusion

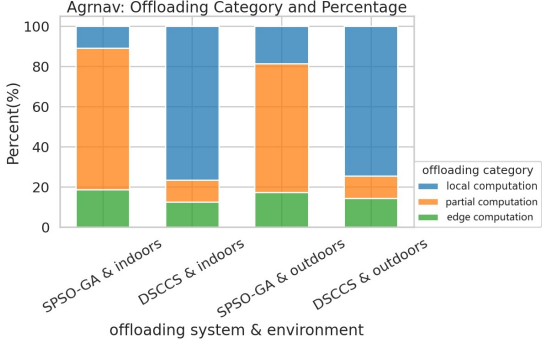
In this paper, we explored the problems that hinder the application of existing parallel methods for distributed inference on robotic IoT, including the failure of data parallelism due

Model(number of parameters)	Environment	Power consumption(W)			Energy consumption(J) per inference <sup>936</sup>		
		Local	SPSO-GA	DSCCS	Local	SPSO-GA	DSCCS <sup>937</sup>
MobileNet_V3_Small (2M)	indoors	6.131( $\pm 0.061$ )	5.448( $\pm 0.168$ )	5.658( $\pm 0.085$ )	0.202( $\pm 0.002$ )	0.241( $\pm 0.107$ )	0.174( $\pm 0.046$ ) <sup>938</sup>
	outdoors	6.131( $\pm 0.061$ )	5.567( $\pm 0.273$ )	5.557( $\pm 0.186$ )	0.202( $\pm 0.002$ )	0.260( $\pm 0.204$ )	0.185( $\pm 0.099$ ) <sup>939</sup>
RegNet_X_3_2GF (15M)	indoors	8.208( $\pm 0.140$ )	5.490( $\pm 0.178$ )	5.714( $\pm 0.342$ )	0.492( $\pm 0.008$ )	0.356( $\pm 0.156$ )	0.278( $\pm 0.091$ ) <sup>940</sup>
	outdoors	8.208( $\pm 0.140$ )	5.878( $\pm 0.659$ )	6.041( $\pm 0.624$ )	0.492( $\pm 0.008$ )	0.406( $\pm 0.295$ )	0.311( $\pm 0.184$ ) <sup>941</sup>
ResNet101 (44M)	indoors	11.851( $\pm 0.404$ )	5.457( $\pm 0.240$ )	5.953( $\pm 0.789$ )	0.711( $\pm 0.024$ )	0.390( $\pm 2.471$ )	0.298( $\pm 0.094$ ) <sup>942</sup>
	outdoors	11.851( $\pm 0.404$ )	6.179( $\pm 1.083$ )	6.431( $\pm 1.060$ )	0.711( $\pm 0.024$ )	0.478( $\pm 0.364$ )	0.349( $\pm 0.216$ ) <sup>943</sup>
ConvNeXt_Base (88M)	indoors	15.335( $\pm 0.273$ )	5.507( $\pm 0.358$ )	7.713( $\pm 2.613$ )	0.721( $\pm 0.013$ )	0.241( $\pm 0.103$ )	0.250( $\pm 0.069$ ) <sup>944</sup>
	outdoors	15.335( $\pm 0.273$ )	7.638( $\pm 3.297$ )	9.148( $\pm 3.338$ )	0.721( $\pm 0.013$ )	0.346( $\pm 0.254$ )	0.307( $\pm 0.171$ ) <sup>945</sup>
ConvNeXt_Large (197M)	indoors	15.403( $\pm 0.082$ )	5.518( $\pm 0.638$ )	6.604( $\pm 2.860$ )	0.786( $\pm 0.004$ )	0.251( $\pm 0.104$ )	0.230( $\pm 0.088$ ) <sup>946</sup>
	outdoors	15.403( $\pm 0.082$ )	8.400( $\pm 4.345$ )	8.895( $\pm 4.505$ )	0.786( $\pm 0.004$ )	0.452( $\pm 0.339$ )	0.366( $\pm 0.248$ ) <sup>947</sup>
RegNet_Y_128GF (644M)	indoors	15.430( $\pm 0.020$ )	5.384( $\pm 1.071$ )	6.151( $\pm 2.155$ )	2.145( $\pm 0.003$ )	1.642( $\pm 0.327$ )	0.615( $\pm 0.216$ ) <sup>948</sup>
	outdoors	15.430( $\pm 0.020$ )	6.361( $\pm 2.349$ )	9.127( $\pm 4.724$ )	2.145( $\pm 0.003$ )	2.748( $\pm 1.015$ )	1.068( $\pm 0.553$ ) <sup>949</sup>

**Table 7.** The power consumption against time (Watt) and energy consumption per inference (Joule) with standard deviation ( $\pm n$ ) of common AI models at different baselines and environments. “Local” represents “Local computation”



**(a)** Categories and percentage of various scheduling for Kapao



**(b)** Categories and percentage of various scheduling for AGRNav

**Figure 6.** The layer partitioning scheduling under difference baselines and environments. “Local computation” refers to placing the whole layers on the robot when the bandwidth is too low, “edge computation” means placing the whole layers on GPU server when the bandwidth is sufficient, and “partial computation” means placing part of the layers on the robot and part on GPU server.

to small batch sizes, the unacceptable communication overhead of tensor parallelism caused by all-reduce communication, and the significant transmission bottlenecks inherent to pipeline parallelism’s scheduling mechanism. By raising awareness of these issues, we aim to stimulate research efforts towards developing novel parallel methods that address these problems. We envision that fast and energy-efficient inference will foster the deployment of diverse robotic tasks on real-world robots in the field.

## References

- [1] [n. d.] iPerf - Download iPerf3 and original iPerf pre-compiled binaries. <https://iperf.fr/iperf-download.php>
- [2] Toni Adame, Marc Carrascosa-Zamacois, and Boris Bellalta. 2021. Time-sensitive networking in IEEE 802.11 be: On the way to low-latency WiFi 7. *Sensors* 21, 15 (2021), 4954.
- [3] Majid Altamimi, Atef Abd Rabou, Kshirasagar Naik, and Amiya Nayak. 2015. Energy cost models of smartphones for task offloading to the cloud. *IEEE Transactions on Emerging Topics in Computing* 3, 3 (2015), 384–398.
- [4] Anh-Quan Cao and Raoul de Charette. 2022. Monoscene: Monocular 3d semantic scene completion. In *Proceedings of the IEEE/CVF Conference on Computer Vision and Pattern Recognition*. 3991–4001.
- [5] Xing Chen, Jianshan Zhang, Bing Lin, Zheyi Chen, Katinka Wolter, and Geyong Min. 2021. Energy-efficient offloading for DNN-based smart IoT systems in cloud-edge environments. *IEEE Transactions on Parallel and Distributed Systems* 33, 3 (2021), 683–697.
- [6] Daniel Crankshaw, Gur-Eyal Sela, Xiangxi Mo, Corey Zumar, Ion Stoica, Joseph Gonzalez, and Alexey Tumanov. 2020. InferLine: latency-aware provisioning and scaling for prediction serving pipelines. In *Proceedings of the 11th ACM Symposium on Cloud Computing*. 477–491.
- [7] Alexandre Défossez, Yossi Adi, and Gabriel Synnaeve. 2021. Differentiable model compression via pseudo quantization noise. *arXiv preprint arXiv:2104.09987* (2021).
- [8] Ming Ding, Peng Wang, David López-Pérez, Guoqiang Mao, and Zihuai Lin. 2015. Performance impact of LoS and NLoS transmissions in dense cellular networks. *IEEE Transactions on Wireless Communications* 15, 3 (2015), 2365–2380.
- [9] Khalid Elgazzar, Patrick Martin, and Hossam S Hassanein. 2014. Cloud-assisted computation offloading to support mobile services. *IEEE*

- 991                    *Transactions on Cloud Computing* 4, 3 (2014), 279–292.
- 992 [10] Zhou Fang, Tong Yu, Ole J Mengshoel, and Rajesh K Gupta. 2017. Qos-aware scheduling of heterogeneous servers for inference in deep neural networks. In *Proceedings of the 2017 ACM on Conference on Information and Knowledge Management*. 2067–2070.
- 993 [11] Stefan Gheorghe and Mihai Ivanovici. 2021. Model-based weight quantization for convolutional neural network compression. In *2021 16th International Conference on Engineering of Modern Electric Systems (EMES)*. IEEE, 1–4.
- 994 [12] Cheng Gong, Yao Chen, Ye Lu, Tao Li, Cong Hao, and Deming Chen. 2020. VecQ: Minimal loss DNN model compression with vectorized weight quantization. *IEEE Trans. Comput.* 70, 5 (2020), 696–710.
- 995 [13] Jianping Gou, Baosheng Yu, Stephen J Maybank, and Dacheng Tao. 2021. Knowledge distillation: A survey. *International Journal of Computer Vision* 129, 6 (2021), 1789–1819.
- 996 [14] Apoorv Gupta, Aman Bansal, and Vidhi Khanduja. 2017. Modern lossless compression techniques: Review, comparison and analysis. In *2017 Second International Conference on Electrical, Computer and Communication Technologies (ICECCT)*. IEEE, 1–8.
- 997 [15] Vinayak Honkote, Dileep Kurian, Sriram Muthukumar, Dibyendu Ghosh, Satish Yada, Kartik Jain, Bradley Jackson, Ilya Klotchkov, Mallikarjuna Rao Nimmagadda, Shreela Dattawadkar, et al. 2019. 2.4 a distributed autonomous and collaborative multi-robot system featuring a low-power robot soc in 22nm cmos for integrated battery-powered minibots. In *2019 IEEE International Solid-State Circuits Conference-(ISSCC)*. IEEE, 48–50.
- 998 [16] Chuang Hu, Wei Bao, Dan Wang, and Fengming Liu. 2019. Dynamic adaptive DNN surgery for inference acceleration on the edge. In *IEEE INFOCOM 2019-IEEE Conference on Computer Communications*. IEEE, 1423–1431.
- 999 [17] Yang Hu, Connor Imes, Xuanang Zhao, Souvik Kundu, Peter A Beerel, Stephen P Crago, and John Paul Walters. 2022. Pipeedge: Pipeline parallelism for large-scale model inference on heterogeneous edge devices. In *2022 25th Euromicro Conference on Digital System Design (DSD)*. IEEE, 298–307.
- 1000 [18] KJ Joseph, Salman Khan, Fahad Shahbaz Khan, and Vineeth N Balasubramanian. 2021. Towards Open World Object Detection. In *Proceedings of the IEEE/CVF Conference on Computer Vision and Pattern Recognition (CVPR)*. 5830–5840.
- 1001 [19] Yiping Kang, Johann Hauswald, Cao Gao, Austin Rovinski, Trevor Mudge, Jason Mars, and Lingjia Tang. 2017. Neurosurgeon: Collaborative intelligence between the cloud and mobile edge. *ACM SIGARCH Computer Architecture News* 45, 1 (2017), 615–629.
- 1002 [20] Nam Sung Kim, Todd Austin, David Baauw, Trevor Mudge, Krisztián Flautner, Jie S Hu, Mary Jane Irwin, Mahmut Kandemir, and Vijaykrishnan Narayanan. 2003. Leakage current: Moore’s law meets static power. *computer* 36, 12 (2003), 68–75.
- 1003 [21] Ang Li, Shuaiwen Leon Song, Jieyang Chen, Jiajia Li, Xu Liu, Nathan R Tallent, and Kevin J Barker. 2019. Evaluating modern gpu interconnect: Pcie, nvlink, nv-sli, nvswitch and gpudirect. *IEEE Transactions on Parallel and Distributed Systems* 31, 1 (2019), 94–110.
- 1004 [22] Qingbiao Li, Fernando Gama, Alejandro Ribeiro, and Amanda Prorok. 2020. Graph neural networks for decentralized multi-robot path planning. In *2020 IEEE/RSJ International Conference on Intelligent Robots and Systems (IROS)*. IEEE, 11785–11792.
- 1005 [23] Yiming Li, Zhiding Yu, Christopher Choy, Chaowei Xiao, Jose M Alvarez, Sanja Fidler, Chen Feng, and Anima Anandkumar. 2023. Voxformer: Sparse voxel transformer for camera-based 3d semantic scene completion. In *Proceedings of the IEEE/CVF Conference on Computer Vision and Pattern Recognition*. 9087–9098.
- 1006 [24] Huanghuang Liang, Qianlong Sang, Chuang Hu, Dazhao Cheng, Xiaobo Zhou, Dan Wang, Wei Bao, and Yu Wang. 2023. DNN surgery: Accelerating DNN inference on the edge through layer partitioning. *IEEE transactions on Cloud Computing* (2023).
- 1007 [25] Bing Lin, Yiniao Huang, Jianshan Zhang, Junqin Hu, Xing Chen, and Jun Li. 2019. Cost-driven off-loading for DNN-based applications over cloud, edge, and end devices. *IEEE Transactions on Industrial Informatics* 16, 8 (2019), 5456–5466.
- 1008 [26] Tao Lin, Lingjing Kong, Sebastian U Stich, and Martin Jaggi. 2020. Ensemble distillation for robust model fusion in federated learning. *Advances in Neural Information Processing Systems* 33 (2020), 2351–2363.
- 1009 [27] Ruofeng Liu and Nakjung Choi. 2023. A First Look at Wi-Fi 6 in Action: Throughput, Latency, Energy Efficiency, and Security. *Proceedings of the ACM on Measurement and Analysis of Computing Systems* 7, 1 (2023), 1–25.
- 1010 [28] Shuai Liu, Xin Li, Huchuan Lu, and You He. 2022. Multi-Object Tracking Meets Moving UAV. In *Proceedings of the IEEE/CVF Conference on Computer Vision and Pattern Recognition (CVPR)*. 8876–8885.
- 1011 [29] Antoni Masiukiewicz. 2019. Throughput comparison between the new HEW 802.11 ax standard and 802.11 n/ac standards in selected distance windows. *International Journal of Electronics and Telecommunications* 65, 1 (2019), 79–84.
- 1012 [30] William McNally, Kanav Vats, Alexander Wong, and John McPhee. 2022. Rethinking keypoint representations: Modeling keypoints and poses as objects for multi-person human pose estimation. In *European Conference on Computer Vision*. Springer, 37–54.
- 1013 [31] Thaha Mohammed, Carlee Joe-Wong, Rohit Babbar, and Mario Di Francesco. 2020. Distributed inference acceleration with adaptive DNN partitioning and offloading. In *IEEE INFOCOM 2020-IEEE Conference on Computer Communications*. IEEE, 854–863.
- 1014 [32] Deepak Narayanan, Mohammad Shoeybi, Jared Casper, Patrick LeGresley, Mostofa Patwary, Vijay Korthikanti, Dmitri Vainbrand, Prethvi Kashinkunti, Julie Bernauer, Bryan Catanzaro, et al. 2021. Efficient large-scale language model training on gpu clusters using megatron-lm. In *Proceedings of the International Conference for High Performance Computing, Networking, Storage and Analysis*. 1–15.
- 1015 [33] Mohammad Noormohammadi and Cauligi S Raghavendra. 2017. Datacenter traffic control: Understanding techniques and tradeoffs. *IEEE Communications Surveys & Tutorials* 20, 2 (2017), 1492–1525.
- 1016 [34] NVIDIA. 2024. The World’s Smallest AI Supercomputer. <https://www.nvidia.com/en-us/autonomous-machines/embedded-systems/jetson-xavier-series/>.
- 1017 [35] Takeshi Ohkawa, Kazushi Yamashina, Hitomi Kimura, Kanemitsu Ootsu, and Takashi Yokota. 2018. FPGA components for integrating FPGAs into robot systems. *IEICE TRANSACTIONS on Information and Systems* 101, 2 (2018), 363–375.
- 1018 [36] Yuanpeng Pei, Matt W Mutka, and Ning Xi. 2013. Connectivity and bandwidth-aware real-time exploration in mobile robot networks. *Wireless Communications and Mobile Computing* 13, 9 (2013), 847–863.
- 1019 [37] Yi Ren, Chih-Wei Tung, Jyh-Cheng Chen, and Frank Y Li. 2018. Proportional and preemption-enabled traffic offloading for IP flow mobility: Algorithms and performance evaluation. *IEEE Transactions on Vehicular Technology* 67, 12 (2018), 12095–12108.
- 1020 [38] Nurul I Sarkar and Osman Mussa. 2013. The effect of people movement on Wi-Fi link throughput in indoor propagation environments. In *IEEE 2013 Tencon-Spring*. IEEE, 562–566.
- 1021 [39] Karen Simonyan and Andrew Zisserman. 2015. Very Deep Convolutional Networks for Large-Scale Image Recognition. arXiv:1409.1556 [cs.CV]
- 1022 [40] Debjyoti Sinha and Mohamed El-Sharkawy. 2019. Thin mobilenet: An enhanced mobilenet architecture. In *2019 IEEE 10th annual ubiquitous computing, electronics & mobile communication conference (UEMCON)*. IEEE, 0280–0285.
- 1023 [41] Sasha Targ, Diogo Almeida, and Kevin Lyman. 2016. Resnet in resnet: Generalizing residual architectures. *arXiv preprint arXiv:1603.08029* (2016).

- 1101 [42] Hao Wang, Sreeram Potluri, Miao Luo, Ashish Kumar Singh, Sayantan  
1102 Sur, and Dhabaleswar K Panda. 2011. MVAPICH2-GPU: optimized  
1103 GPU to GPU communication for InfiniBand clusters. *Computer Science-  
1104 Research and Development* 26, 3 (2011), 257–266.
- 1105 [43] Junming Wang, Zekai Sun, Xiuxian Guan, Tianxiang Shen, Zongyuan  
1106 Zhang, Tianyang Duan, Dong Huang, Shixiong Zhao, and Heming Cui.  
2024. AGRNav: Efficient and Energy-Saving Autonomous Navigation  
1107 for Air-Ground Robots in Occlusion-Prone Environments. In *IEEE  
1108 International Conference on Robotics and Automation (ICRA)*.
- 1109 [44] Lin Wang and Kuk-Jin Yoon. 2021. Knowledge distillation and student-  
teacher learning for visual intelligence: A review and new outlooks.  
*IEEE transactions on pattern analysis and machine intelligence* 44, 6  
1110 (2021), 3048–3068.
- 1111 [45] Sanghyun Woo, Shoubhik Debnath, Ronghang Hu, Xinlei Chen,  
1112 Zhuang Liu, In So Kweon, and Saining Xie. 2023. Convnext v2: Co-  
1113 designing and scaling convnets with masked autoencoders. In *Proceedings of the IEEE/CVF Conference on Computer Vision and Pattern  
1114 Recognition*. 16133–16142.
- 1115 [46] Huaming Wu, William J Knottenbelt, and Katinka Wolter. 2019. An  
1116 efficient application partitioning algorithm in mobile environments.  
*IEEE Transactions on Parallel and Distributed Systems* 30, 7 (2019),  
1464–1480.
- 1117 [47] Tianyu Wu, Shizhu He, Jingping Liu, Siqi Sun, Kang Liu, Qing-Long  
1118 Han, and Yang Tang. 2023. A brief overview of ChatGPT: The history,  
status quo and potential future development. *IEEE/CAA Journal of  
1119 Automatica Sinica* 10, 5 (2023), 1122–1136.
- 1120  
1121  
1122  
1123  
1124  
1125  
1126  
1127  
1128  
1129  
1130  
1131  
1132  
1133  
1134  
1135  
1136  
1137  
1138  
1139  
1140  
1141  
1142  
1143  
1144  
1145  
1146  
1147  
1148  
1149  
1150  
1151  
1152  
1153  
1154  
1155
- 1156 [48] Zhaoyang Xia, Youquan Liu, Xin Li, Xinge Zhu, Yuexin Ma, Yikang Li,  
Yuenan Hou, and Yu Qiao. 2023. SCPNet: Semantic Scene Completion  
1157 on Point Cloud. In *Proceedings of the IEEE/CVF Conference on Computer  
1158 Vision and Pattern Recognition*. 17642–17651.
- 1159 [49] Yecheng Xiang and Hyoseung Kim. 2019. Pipelined data-parallel  
1160 CPU/GPU scheduling for multi-DNN real-time inference. In *2019 IEEE  
1161 Real-Time Systems Symposium (RTSS)*. IEEE, 392–405.
- 1162 [50] Jing Xu, Yu Pan, Xinglin Pan, Steven Hoi, Zhang Yi, and Zenglin Xu.  
2022. RegNet: self-regulated network for image classification. *IEEE  
1163 Transactions on Neural Networks and Learning Systems* (2022).
- 1164 [51] Min Xue, Huaming Wu, Guang Peng, and Katinka Wolter. 2021.  
DDPQN: An efficient DNN offloading strategy in local-edge-cloud  
1165 collaborative environments. *IEEE Transactions on Services Computing*  
1166 15, 2 (2021), 640–655.
- 1167 [52] Xinlei Yang, Hao Lin, Zhenhua Li, Feng Qian, Xingyao Li, Zhiming He,  
Xudong Wu, Xianlong Wang, Yunhao Liu, Zhi Liao, et al. 2022. Mobile  
access bandwidth in practice: Measurement, analysis, and implications.  
In *Proceedings of the ACM SIGCOMM 2022 Conference*. 114–128.
- 1168 [53] Yang Yang, Li Juntao, and Peng Lingling. 2020. Multi-robot path  
1169 planning based on a deep reinforcement learning DQN algorithm.  
*CAAI Transactions on Intelligence Technology* 5, 3 (2020), 177–183.
- 1170 [54] Yonghao Zhuang, Hexu Zhao, Lianmin Zheng, Zhuohan Li, Eric Xing,  
Qirong Ho, Joseph Gonzalez, Ion Stoica, and Hao Zhang. 2023. On  
optimizing the communication of model parallelism. *Proceedings of  
Machine Learning and Systems* 5 (2023).
- 1171  
1172  
1173  
1174  
1175  
1176  
1177  
1178  
1179  
1180  
1181  
1182  
1183  
1184  
1185  
1186  
1187  
1188  
1189  
1190  
1191  
1192  
1193  
1194  
1195  
1196  
1197  
1198  
1199  
1200  
1201  
1202  
1203  
1204  
1205  
1206  
1207  
1208  
1209  
1210